Special Section:
Critical Zone Observatories

A. Swarowsky
R.A. Dahlgren
K.W. Tate
J.W. Hopmans
A.T. O'Geen*

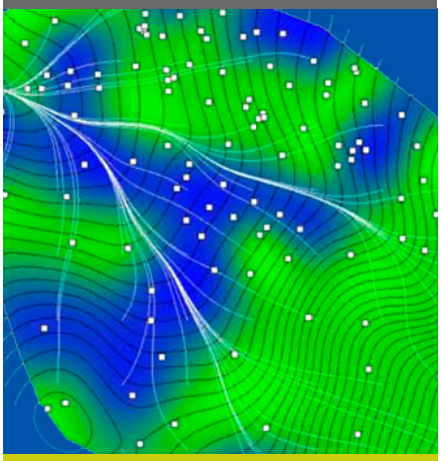

Climate, subsurface lateral flow, streamflow, and soil moisture (100 pedons) were monitored in a headwater catchment in northern California. Results identified four seasonally dependent drivers of soil moisture status and subsequent catchment hydrology including vegetation (oak tree vs. grassland), horizon stratigraphy, aspect, and topography.

A. Swarowsky, Soils and Biogeochemistry Graduate Group, Univ. of California, Davis, CA 95616; R.A. Dahlgren, J.W. Hopmans, and A.T. O'Geen, Dep. of Land, Air, and Water Resources, Univ. of California, One Shields Ave., Davis, CA 95616; K.W. Tate, Dep. of Plant Sci., Univ. of California, Davis, CA 95616. *Corresponding author (atogeen@ucdavis.edu).

Vadose Zone J. 10:800–815
doi:10.2136/vzj2010.0126
Received 26 Oct. 2010.
Posted online 29 July 2011.

Catchment-Scale Soil Water Dynamics in a Mediterranean-Type Oak Woodland

Water availability is one of the most serious natural resource issues facing California, especially given projections for future climate change. The 3 million ha of oak (*Quercus* spp.) woodlands play a critical role in California's water supply system, providing runoff primarily from winter rainfall events and hosting two-thirds of the state's drinking water reservoirs. Thus, understanding water storage and streamflow regulation by soils in these watersheds is essential for water resource planning under future climate change scenarios. The primary objectives of this research were to identify the drivers of soil moisture dynamics and the hydrologic budget at the catchment scale and their relationships with streamflow generation. A 33-ha headwater catchment in the Sierra Nevada foothills of northern California was instrumented to monitor climate, subsurface lateral flow, streamflow, and soil moisture within 100 pedons distributed throughout the catchment. A catchment-scale water balance was used to examine factors regulating spatial and temporal soil water distribution within the catchment. Relationships between soil, topographic, and vegetation characteristics and soil water content at each pedon were analyzed using a linear mixed-effects model with four fixed effects: vegetation type or cover, presence or absence of a claypan, compound topographic index, and solar radiation. Streamflow was limited to periods when lower soil horizons were at or near saturation. Following saturation, each rainfall event generated subsurface lateral flow above the clay-rich argillic horizon, resulting in sharp hydrograph responses with little base flow between rainfall events. For the two water years examined, 9.6 and 11.5% of rainfall left the catchment as streamflow. Vegetation (tree vs. grassland), presence or absence of a claypan, aspect, and compound topographic index (index of wetness) were all significantly correlated to soil moisture status and thus streamflow generation at various times throughout the year. Findings indicated that watershed-scale hydrologic models based solely on surface topography will not fully explain dynamic temporal and spatial variability in hydrologic flow paths and streamflow generation in these oak woodland catchments. In particular, watershed-scale knowledge of soil stratigraphy (e.g., claypan distribution) was important for understanding catchment hydrology, especially the occurrence of subsurface lateral flow dynamics.

Abbreviations: CTI, compound topographic index; DD, dry-down; ET, evapotranspiration; FW, full wet; QW, quasi-wet; SD, summer dry; SWC, soil water content; WU, wet-up.

The availability of clean water is arguably one of the most important resource issues facing the global community (National Geographic Society, 2010). Fundamental to our knowledge of water resources is the role of the soil system as a natural reservoir having the capacity to store and supply water for streamflow and biota. This knowledge is essential for understanding ecosystem dynamics and biogeochemical cycles of both terrestrial and downstream aquatic ecosystems (Moehrlen et al., 1999; Chamran et al., 2002). An emerging issue in hydrology and critical zone research is to describe and explain the spatial and interannual variability of soil moisture storage and its effects on the soil water balance and streamflow generation. This type of investigation can be used to explain, for example, the partitioning of precipitation into evapotranspiration and runoff. Furthermore, understanding soil water storage is important because a variety of widely used hydrologic models depend on the soil water budget, such as SWAT, PEARL, and SESOIL (Pistocchi et al., 2008).

The complexity involved in ecosystem water balance estimation is well known and involves quantification of rainfall, canopy interception, evapotranspiration, streamflow, deep percolation, and changes in soil water storage. The principal methods of assessing the water balance usually involve annual cumulative measurements of precipitation input, evapotranspiration, and runoff, and, by difference, the annual change in soil water storage is inferred. Although a variety of studies have described the water balance at different scales and climatic conditions (Joffre and Rambal, 1993; Huang, 1997; Lewis et al., 2000;

Moehrlen et al., 1999), few have rigorously evaluated the seasonal importance and dynamics of soil water storage in the overall water balance at the catchment scale (Milly, 1994). Storage is inferred because it is often assumed that changes in soil water storage with time are relatively insignificant compared with changes in rainfall and runoff. Because arid and semiarid environments are characterized by a strong seasonally dynamic moisture regime (Major, 1988; Lewis et al., 2000), however, changes in water storage with time can be quite dramatic within relatively short periods of time.

Previous studies in oak woodland watersheds have demonstrated tremendous variability in annual runoff/rainfall ratios, which ranged from 0.19 to 0.76 during a 17-yr record (Lewis et al., 2000). Other studies have highlighted the importance of complex interactions between soils and plants in regulating soil moisture storage during the year. For example, the water balance in open grasslands compared with under an oak tree canopy can differ by 50% (Joffre and Rambal, 1993; Huang, 1997); soil properties are very different under oak than open grasslands (Dahlgren et al., 1997, 2003) and soil water loss through evapotranspiration can also be higher under oak than grasslands (Jackson et al., 1990; Dahlgren and Singer, 1994; Black, 1996).

The climatic variability intrinsic to semiarid Mediterranean environments makes the evaluation of changes in soil water storage difficult. Soil moisture change during hourly to seasonal time periods is necessary to document to fully understand the hydrologic behavior in headwater catchments of these systems. Implementation of a program to monitor soil moisture storage must necessarily involve a large number of sensors to adequately and continuously cover the catchment's water storage in four dimensions (time, depth, and x–y space).

We established a comprehensive hydrologic monitoring infrastructure within an experimental headwater catchment to measure the interplay between climate, soil moisture dynamics, subsurface lateral flow, and streamflow. The primary objectives of this research were to identify the drivers of soil moisture dynamics at the catchment scale and document the hydrologic budget. The following questions were addressed, considering annual variability of soil moisture:

1. How does vegetation (oak trees vs. annual grasslands) influence soil water storage?
2. How does the occurrence of a claypan influence water storage and flow?
3. How do solar radiation and surface topography influence soil water storage?

Materials and Methods

Catchment Characteristics

The experimental catchment is located at the University of California's Sierra Foothill Research and Extension Center (SFREC) in Yuba County in northern California (Fig. 1). The catchment area is 33 ha, with a mean elevation of 282 m, a relief of 227 m, and southeast to northwest orientation. Slopes range from near 0 to approximately 32°. An ephemeral stream drains the catchment in the winter and spring.

The climate is Mediterranean, with cool, moist winters and hot, dry summers. The mean annual air temperature is 15°C (January mean of 8.4°C; July mean of 25.9°C). Annual precipitation averages 740 mm (307–1235 mm during the past 20 yr) and falls exclusively as rainfall, primarily between November and March. Annual potential evaporation measured by pan evaporation at SFREC is 1343 mm (Snyder et al., 1985).

Vegetation varies from oak savanna on southeast-facing hillslopes to dense oak woodlands on northwest-facing slopes. Canopy coverage was 66% estimated from digital imagery (1-m resolution) and field reconnaissance (Fig. 2). Blue oak (*Quercus douglasii* Hook & Arn.) is the dominant tree species, with a minor component of interior live oak (*Quercus wislizeni* DC.) and foothill pine (*Pinus sabiniana* Douglas). The oak understory and open grassland communities are dominated by annual grasses (Jackson et al., 1990).

Soils are formed from Jurassic meta-igneous and metasedimentary rocks of the Smartville complex, which is a rifted volcanic arc consisting of igneous basement and fragments of its post-volcanic sedimentary cover from a section of oceanic crust (Beiersdorfer, 1987). Bedrock characteristics are highly variable in space, ranging from strongly consolidated to highly fractured across the landscape. Two soil types are present in the catchment: Palexeralfs (soils with claypans), found at lower slope positions (level benches and landforms that gather water), and Haploxeralfs (soils without claypans), found at convex and steeply sloping linear upland positions (Fig. 2).

Monitoring Infrastructure

The catchment monitoring infrastructure (Fig. 1) measured the following hydrologic parameters: climate (precipitation, air temperature, relative humidity, incoming solar radiation, wind speed, and soil temperature at a 5-cm depth), subsurface lateral flow, streamflow, and soil moisture. All meteorologic data were collected on an hourly basis by an automated weather station. A perched water collection system (PWCS), excavated to bedrock, was constructed to measure the subsurface lateral flow from four different soil horizons in triplicate soil profiles. As part of the PWCS, collection gutters were inserted at the lower boundary of the A (10 cm), AB (25 cm), and Bt1 (65 cm) horizons and the C horizon–saprolite interface (100–110 cm). Subsurface lateral flow was directed to tipping buckets connected to dataloggers to calculate volumetric flow rates from each soil horizon. Streamflow was measured using a gauging station equipped with a Parshall flume for high flows and a 90° V-notch weir for low flows to maximize monitoring accuracy. Stage height was measured at 15-min intervals using an electronic stage sensor (AGS Aquatape, JOWA USA, Littleton,

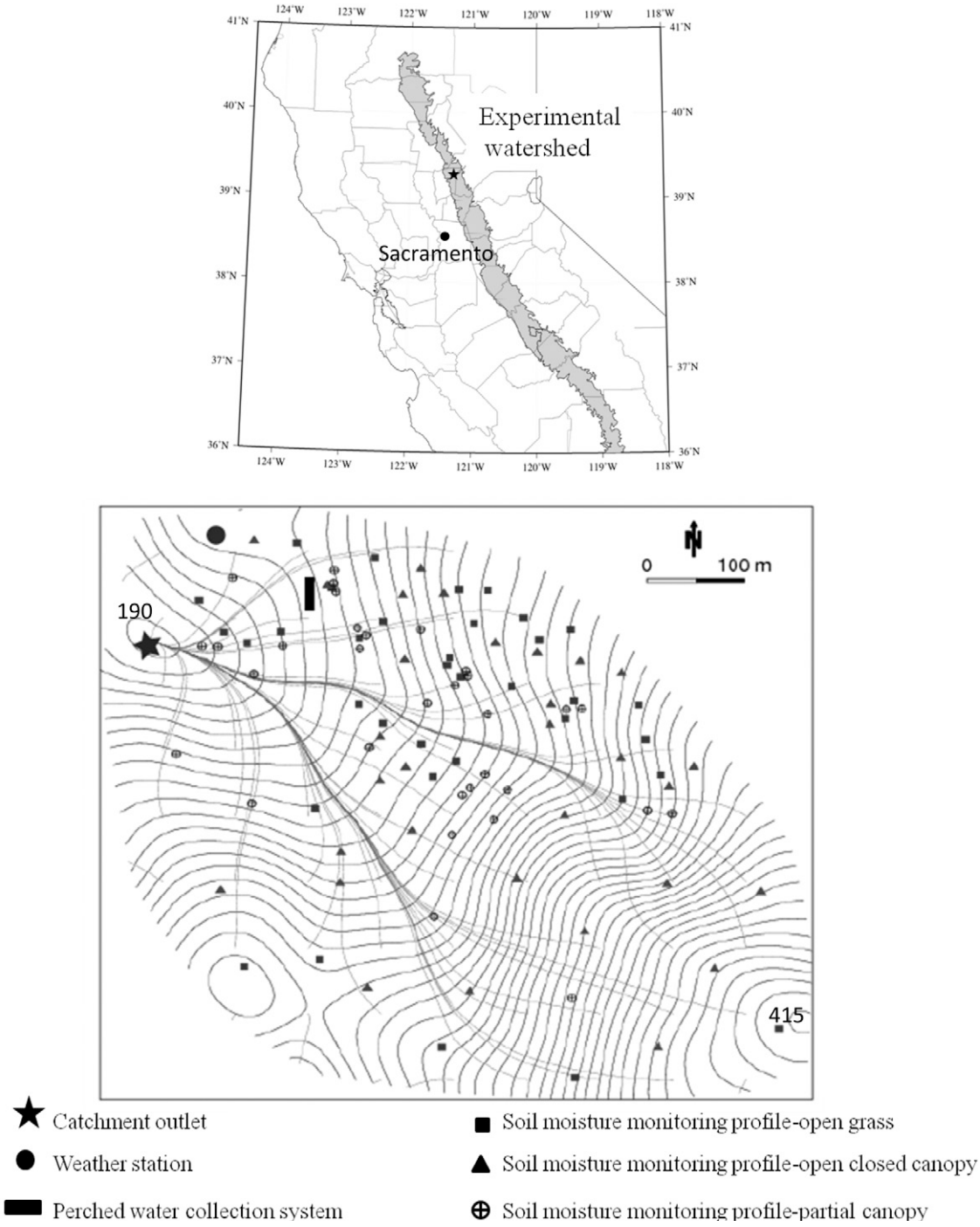

Fig. 1. Location of the experimental catchment at the Sierra Foothill Research and Extension Center. The 5-m topographic map depicts the monitoring infrastructure. Flow density lines (perpendicular intersects of contour lines) depict an estimation of flow direction.

MA) recorded with a datalogger. Stage–discharge relationships were determined using standard rating equations. Calibration of the electronic stage sensor was performed at the onset of the rainy season and periodically verified during runoff events.

Soil moisture was recorded throughout the catchment with capacitance soil moisture probes (ECH_2O probes, Decagon Devices, Pullman, WA) in 100 soil profiles beginning in November 2006. Monitoring locations were chosen based on the following criteria: (i) spatial distribution (maximal coverage); (ii) vegetation characteristics, including under trees, open grassland, and partial canopy at least 3 m from the trees in open grass areas; (iii) topography (concave vs. convex) and aspect (north vs. south); and (iv) hydraulically contrasting soils (Palexeralfs and Haploxeralfs) (Fig. 2). During sensor installation, soil profiles (n = 100) were described and sampled according to standard soil survey techniques. Physical (e.g., texture)

and morphological (e.g., abrupt boundaries) characterization techniques were used to identify the presence (Palexeralfs) or absence (Haploxeralfs) of claypans (among other features) in the watershed. Three depths were chosen for sensor placement based on the presence of major genetic horizons, which differed between the Palexeralfs and Haploxeralfs (Table 1): (i) at 10 cm, the A–AB interface; (ii) at 30 cm the upper boundary of the argillic horizon; and (iii) at 50 cm, the middle of the argillic (Haploxeralfs) or upper boundary of the claypan if present (Palexeralfs). While the upper boundary of the claypan was commonly at 50 cm, this sensor was always placed at the upper boundary of the claypan and the exact depth varied accordingly. The fourth sensor was placed according to the following dominant horizon conditions: directly within the claypan if present, or at the solum–Cr horizon interface if no claypan was observed. Although we chose to use common depths to place the upper two sensors (10 and 30 cm), these depths reflect similarities in soil stratigraphic relationships that were determined during the mapping efforts within the catchment. The AB horizons displayed gradual or diffuse horizon boundaries that complicated the interpretation of mean depth reported in Table 1 and our reasoning for placing sensors at 30 cm. In general, the upper 30 cm of soil reflected a strikingly common soil stratigraphic sequence of well-mixed soil biomantle (by gophers) having similar morphologic and physical properties. The sensor designated as 50-cm depth was always placed at that depth

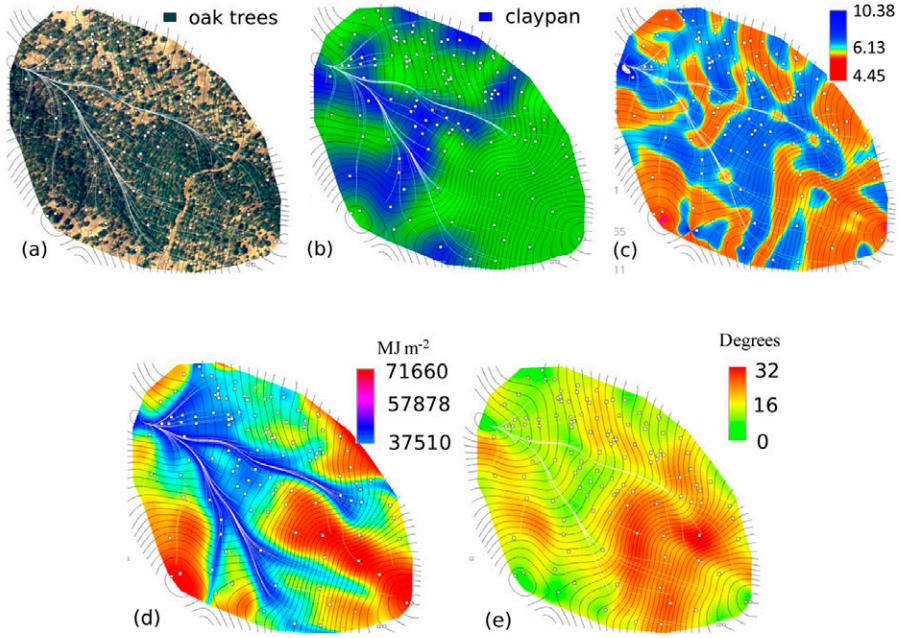

Fig. 2. Tree density (a) interpolated distribution of soils with claypans (b), compound topographic index (CTI) (c), solar radiation model (d), and slope (e) estimated from a 5-m digital elevation model. Flow density lines in (a) are shown in white. Contour lines (5-m) are depicted in gray. White points represent the location of the soil moisture monitoring profiles. Maps (a), (b) and (e) are presented as descriptive information and were not used in the statistical comparisons.

Table 1. Soil physical properties for two representative pedons (a Palexeralf and a Haploxeralf) in the experimental catchment.

Soil	Horizon	Depth		Sand	Silt	Clay	Cf‡	D_b§	K_{sat}¶	
		Mean	SD†						Horizontal	Vertical
		cm		%				g cm^{-3}	cm min^{-1}	
Haploxeralf	A	0–10	3	33.1	42.3	24.6	10	1.3	0.18 (0.11)#	0.16 (0.10)
	AB	10–25	11	30.9	42.4	26.7	15	1.4	0.08 (0.04)	0.21 (0.10)
	Bt1	25–52	14	26.3	35.7	38.1	30	1.6	0.05 (0.07)	0.03 (0.02)
	Bt2	52–85	14	23.2	33.1	43.8	30	1.7	0.04 (0.003)	0.03 (0.03)
	Bt3	85–108	10	26.6	35.1	38.4	30	1.7	0.04 (0.04)	0.01 (0.01)
	Crt	108–146	20	28.9	30.2	40.9	–	1.8	–	–
	R	>146	–	–	–	–	–	–	–	–
Palexeralf	A	0–8	3	39.2	43.8	17.1	10	1.1	1.4 (1.2)	0.21 (0.22)
	AB	8–20	8	38.0	43.7	18.3	15	1.5	0.09 (0.03)	0.25 (0.06)
	Bt1	20–32	10	35.2	42.3	22.5	30	1.6	0.05 (0.07)	0.03 (0.02)
	Bt2	32–52	10	31.5	35.7	32.8	30	1.9	0.02 (0.004)	0.04 (0.04)
	2Btss	52–70	16	23.5	28.8	47.7	10	1.7	0.001 (0.0003)	0.005 (0.004)
	2Crt	70–86	16	42.0	29.9	28.1	–	–	–	–
	2R	>86	–	–	–	–	–	–	–	–

† Standard deviation of depth of the lower boundary of each horizon.
‡ Coarse fragments >2 mm.
§ Bulk density.
¶ Saturated hydraulic conductivity.
# Mean with SD in parentheses.

for Haploxeralfs (~80% of the profiles) but varied slightly in depth for the Palexeralfs, where this sensor was placed at the upper boundary of the claypan. Thus the 50-cm depth represents the upper half of the argillic (Bt1) in Haploxeralfs, which was similar across the catchment because of the degree of mixing. The 70-cm depth was chosen to represent one of two hypothesized conditions, the slowly permeable conditions within the claypan or the potential impermeable nature of the saprolite and bedrock.

The vegetation canopy condition was measured at each profile. The assessment consisted of three different categories: (i) closed, soil profiles directly under an oak canopy; (ii) open, soil profiles within a grassland patch at least 10 m from any oak canopy; and (iii) partial, soil profiles within a wooded area, but not directly under a single oak canopy, i.e., within 3 m of an oak canopy.

Sensors were connected to Campbell CR1000 (Campbell Scientific, Logan, UT) or Decagon em5b (Decagon Devices) dataloggers to measure volumetric water content at 5-min intervals and were recorded as 15-min averages. Before installation, the sensors were calibrated to volumetric water content using representative soils from the watershed (Kizito et al., 2008). Sensor accuracy after calibration was about ±5%, in agreement with sensor specifications. Soil moisture data used in this study were from the 2007–2008 and 2008–2009 water years (October–September).

The Water Balance Approach

A catchment-scale water balance was used to examine the factors regulating spatial and temporal soil water distribution within the catchment:

$$E_A = P - R - \Delta S - D \quad [1]$$

where E_A is actual evapotranspiration, P is precipitation, R is stream discharge, ΔS is the change in soil water storage, and D is deep seepage. Because precipitation, stream discharge, and soil water storage were measured, the sum of evapotranspiration (ET) and deep seepage was estimated from the water balance (Ceballos and Schnabel, 1998). Deep seepage was assumed to occur only during the winter when the lower soil horizons were at or near saturation and when transpiration by vegetation was minimal. Thus ET and deep seepage were partitioned assuming that ET in winter was the result of canopy interception (23% by trees and 10% by grasslands) during rainfall events (Dahlgren et al., 1997). The remainder of the combined ET and deep seepage term was assumed to be just deep seepage. Surface runoff was assumed to be negligible based on the results from 13 runoff collectors installed throughout the catchment that rarely collected water. When surface runoff was recorded, it occurred as saturated overland flow in isolated areas distal to the stream.

Soil water storage (θ_{vs}, m^3) for a given depth interval and area of influence was determined using the soil moisture network (100 pedons) and was calculated as

$$\theta_{vs} = \theta_v(z)(a)(1 - Cf) \quad [2]$$

where θ_v is the measured water content ($m^3\ m^{-3}$), z is the representative depth of influence of the sensor (m), a is the horizontal area of influence (m^2) determined by Thiessen polygons (also termed Voronoi polygons), and Cf is the coarse fragment (>2-mm fraction) content.

All values for storage in each depth increment and area of horizontal influence were summed to estimate the total soil water storage of the catchment. The depth of influence for each sensor was assumed to reflect the soil moisture content within genetic horizons. The boundaries of Thiessen polygons were mathematically defined by the perpendicular bisectors of the lines between all the points of interest and surrounding points (Hayes and Koch, 1984).

Statistical Analysis of Water Content and Watershed Characteristics

The relationships between soil, solar radiation, compound topographic index (CTI), and oak canopy coverage with soil water content (SWC) were determined using linear mixed-effects regression analysis (Lindstrom, and Bates, 1990; R Development Core Team, 2009; Pinheiro et al., 2009). Independent fixed effects included in the analysis were vegetation cover, the presence or absence of a claypan (Palexeralfs vs. Haploxeralfs), CTI, and solar radiation determined at the position of each pedon. The values of CTI and solar radiation were selected from a preliminary analysis as the most significant factors related to soil moisture from a suite of variables interpolated from a digital elevation model (DEM), such as slope steepness, terrain characterization index, surface curvature, and Llobera's topographic prominence index. Soil water content ($m^3\ m^{-3}$) was the dependent variable in the analysis. Repeated measurements of soil moisture at each pedon introduced autocorrelation into the data, which violates the assumption of independence inherent in linear regression analysis. Extending the linear regression model to include the random intercept term pedon identity (1–100) accounted for the autocorrelation and satisfied the assumption of independence.

Soil water storage, as computed from SWC measurements, was analyzed for five defined time periods, representing seasonal climatic differences and important hydrologic transitions. For statistical analysis, we grouped the soil moisture data from the top two sensors (here referred to as the near-surface biomantle) and the bottom two sensors (here referred to as the subsurface argillic horizon). These groupings reflect important morphologic differences, such as the actively churned and porous biomantle and the more stable argillic horizon. The near-surface biomantle and the subsurface argillic horizon reflect the average volumetric soil moisture contents of the 10- to 30- and the 50- to 70-cm depths, respectively, for each seasonal soil moisture state. Thus, a total of four linear mixed-effects analyses (four independent fixed effects

measured at each soil profile) were conducted for two soil depths during five time periods. A post-hoc Tukey test was used to determine the differences within each significant ($P < 0.05$) fixed effect.

Solar radiation was evaluated at each point using the European Solar Radiation Atlas clear-sky model for shortwave solar radiation (Beaudette and O'Geen, 2009). This model computed an integrated index of solar radiation based on aspect, slope, shading, and atmospheric clarity and was used to classify each location as either "north" (37,510–57,878 MJ m^{-2} yr^{-1}) or "south" (57,879–71,660 MJ m^{-2} yr^{-1}) (Beaudette and O'Geen, 2009). The CTI was derived from a 5-m DEM (Moore et al., 1991; 1993). This index is a function of both slope and upstream contributing area per unit width orthogonal to the flow direction:

$$\mathrm{CTI} = \ln\left(\frac{\mathrm{As}}{\tan\beta}\right)$$

where As is the specific catchment area (m^2 m^{-1}) and β is the slope angle in degrees.

This numerical integrated index of topography was used to classify locations as either "lowland" (4.45–6.13) or "upland" (6.13–10.38) for each point. The spatial distributions of claypan, solar radiation index, and CTI in the catchment are shown in Fig. 2.

Results and Discussion

Soil Properties

Soils with claypans (Palexeralfs) were characterized by the following horizon sequence: A–AB–Bt1–Bt2–2Btss–2Crt–2R (Table 1). The claypan (2Btss horizon) often contained >50% clay and increased abruptly at the upper boundary, located 50 to 70 cm below the soil surface. In contrast, Haploxeralfs were characterized by Bt horizons in place of the claypan, with the following horizon sequence: A–AB–Bt1–Bt2–Bt3–Crt–R (Table 1). The surface horizons (A and AB) were similar for both soil types, with loamy soil textures (17–27% clay). Moreover, the bulk density was relatively low in the A and AB horizons (1.1–1.5 g cm^{-3}) of both soils and increased in the subsurface horizons (1.6–1.9 g cm^{-3}). In the Palexeralfs, the vertical saturated hydraulic conductivity (K_{sat}) decreased with depth by two orders of magnitude, ranging from 0.21 cm min^{-1} in the A horizon to 0.005 cm min^{-1} in the 2Btss horizon (claypan). The vertical K_{sat} values for the Haploxeralfs were similar to the Palexeralfs in the upper horizons (~0.2 cm min^{-1}); however, K_{sat} values for the Bt horizons (0.03 cm min^{-1}) were higher than for the claypan (0.005 cm min^{-1}). The high K_{sat} values of the A horizons was consistent with the lack of observable surface runoff. The soil depth for both soil types ranged from 75 and 150 cm, with a saprolite layer overlying bedrock. The bedrock ranged from strongly consolidated and unfractured to highly fractured across the catchment, resulting in zones with both high and low bedrock permeability.

Rainfall, Soil Moisture, and Runoff Characteristics

A total of 489 and 610 mm of rainfall was recorded for the 2007–2008 and 2008–2009 water years (starting 1 October), respectively, compared with the long-term mean of 740 mm. Following the summer periods, during which the pedons were dry, 193 and 195 mm of cumulative rainfall in the 2007–2008 and 2008–2009 water years were required to recharge the soil moisture to the point of generating stream runoff. The progression of the wetting front from upper to lower soil horizons was evident in fall and early winter (Fig. 3). Streamflow was initiated in early January once the subsoil approached saturation. Subsurface lateral flow through the A, AB, and Bt horizons occurred in synchrony with streamflow after the lower B horizons were saturated. For the remainder of the wet season, the B horizons remained at or near saturation while the water contents of the A and AB horizons fluctuated after each rainfall and subsequent drainage event (Fig. 3). Fluctuation in water content in upper soil horizons is a reflection of perched water table dynamics above the claypan. These soil hydrologic characteristics mimicked the stream hydrograph response to rainfall events, being flashy with sharp rising and falling limbs, short peak flows, and the absence of base flow between storms (Fig. 3). For most rainfall events, >80% of the total runoff volume was recorded during a 1-h period. Following cessation of rainfall in late spring, the soil profiles typically dried throughout the summer period (Fig. 3 and 4).

Classification of Soil Moisture States during the Hydrologic Year

Based on the relationships among precipitation, soil moisture, subsurface lateral flow, and streamflow, five soil moisture states were identified to partition the hydrologic year: fall wet-up (WU), quasi-wet (QW), full wet (FW), dry-down (DD), and summer dry (SD) (Table 2). These states were based on similar observations in other studies that described seasonally contrasting hydrologic conditions (Huang, 1997; Black, 1996; Grayson et al., 1997; McNamara et al., 2005). The WU state was defined by the onset of precipitation in October. In this soil moisture state, the storage capacity of the soils was recharged following the SD period. During the WU state, the wetting front advanced downward in the profile, depending on infiltration in excess of evapotranspiration. In the WU state, stream discharge did not respond to rainfall events (Fig. 3). After the WU state, the first streamflow event of the year represented the transition to the wet soil moisture periods (QW and FW), during which all streamflow events occurred.

Substantial changes in soil water storage occurred during the first few storms of each year—without any subsurface lateral flow, however. This period of soil wetting was in contrast to the subsequent FW state when no further soil water storage changes occurred with later storms, and lateral flow was initiated (Fig. 3). Therefore, we classified the soil wetting period into early (QW) and a late (FW) soil moisture states. The

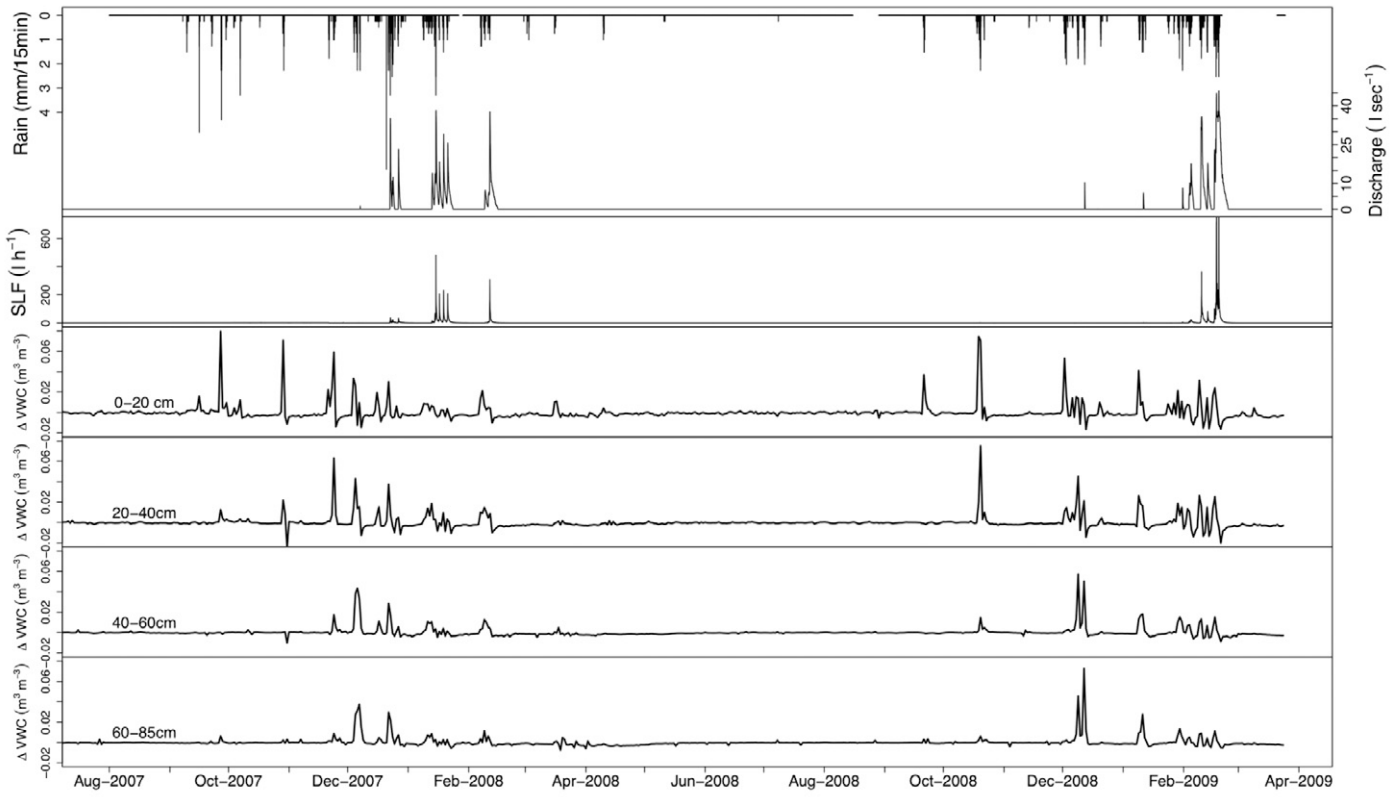

Fig. 3. Rainfall, runoff, subsurface lateral flow (SLF) and daily change in soil water content (ΔVWC) in the experimental catchment for the 2007–08 and 2008–09 monitoring years. Each peak or pulse in ΔVWC represents a daily additional increase or decrease in water content. The upper boundary of the claypan is located in the 40–60 cm layer (Table 1). SLF is total subsurface lateral flow from all horizons.

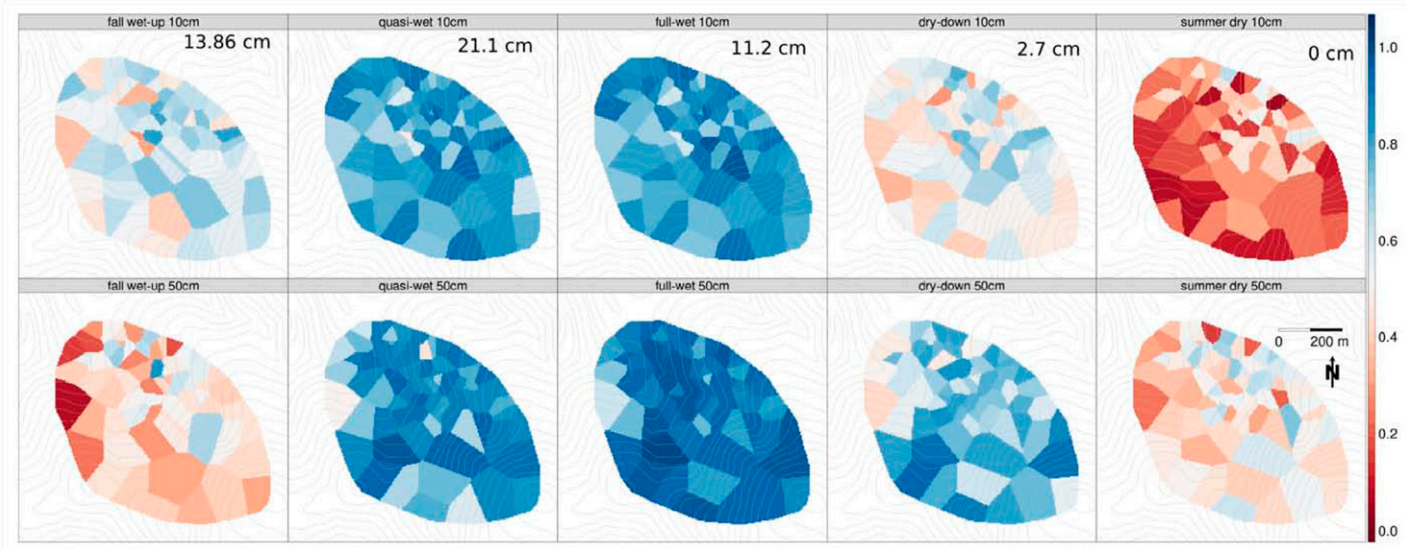

Fig. 4. Spatial patterns in mean seasonal percentage of saturation (moisture content divided by the highest value observed in the state) summarized at 10 and 50 cm depths for the five states in the 2007–2008 water year. Values in the upper panel for each state represent cumulative rainfall.

transition between these two states was indicated by the onset of subsurface lateral flow that occurred when the soils were at or near saturation and there was no change in soil water storage with each subsequent rainfall event.

The DD state was marked by the lack of stream runoff during rainfall events. Occasional rainfall maintained the soil water storage, but overall, soil water was lost to ET. The SD period was defined based on high temperatures, the absence of rainfall, and an imperceptible change in daily soil moisture content. The transition

Table 2. Differentiating criteria for soil moisture states observed from patterns in climate, soil moisture, stream discharge, and lateral subsurface flow.

Soil moisture state	Differentiating characteristics
Summer dry	soils are uniformly dry throughout profile; imperceptible daily changes in soil water content
Fall wet-up	onset of the rainy season; no stream discharge observed; subsurface layers (below 50 cm) remain dry
Quasi-wet	stream discharge occurs during storm events; subsurface lateral flow begins but only in select horizons
Full wet	stream discharge occurs during storm events; subsurface lateral flow occurs in several horizons; clay-rich layers are at or near saturation
Dry-down	stream discharge ceases to occur even in response to storm events; loss of soil moisture, especially in upper 30 cm

from DD to the SD state corresponded with a decrease in the daily change in SWC in early May (Fig. 3). These states were used to compare the components of the water balance and analyze the effects of catchment parameters on soil moisture dynamics.

Seasonal Trends in Watershed Soil Water Content

Seasonal trends in soil moisture content showed distinct differences across the watershed between surface and subsurface horizons for the five soil moisture states (Fig. 4). During WU, soil moisture primarily increased in surface horizons (Tables 3 and 4; Fig. 3 and 4), although macropore flow through root channels and krotovinas may have contributed to some preferential wet-up in lower soil horizons. During the QW and FW states, the upper soil horizons approached saturation and there was little difference in the degree of soil saturation between the states. In contrast, while the deeper horizons wet up substantially during the QW state, these layers didn't fully saturate until the FW state (Tables 3 and 4; Fig. 3 and 4). During the FW state, the distribution of saturated conditions at 50 cm appearred to loosely reflect the patterns of water accumulation identified by the CTI (Fig. 2c and 4). This perceived weak relationship with topography is inconsistent other studies (e.g., Grayson et al., 1997) that have described how wetness dynamics are related to the upslope contributing area.

During the DD state, soil moisture depletion was greatest in the surface horizons (upper 20 cm) relative to the deeper soil horizons (Fig. 3). The total amount of water lost was similar among horizons (30–36 mm), however, owing to differences in water holding capacity (Tables 1, 3, and 4). This trend continued into the SD state when the surface horizons became severely desiccated (generally <30% of saturation), while the lower horizons were depleted to between about 40 to 60% of saturation. Shallow-rooted (upper 40 cm) annual grasses die by late May, although oak trees have roots distributed throughout the soil profile and continue to extract water throughout the summer (Millikin Ishikawa and Bledsoe, 2000; Baldocchi and Xu, 2007).

Seasonal Water Balance

The dynamics of water storage differed markedly between states. During WU, recharge primarily occurred in the surface horizons (0–40 cm) and represented 70 to 91% of the total recharge of soil moisture for the WU state (Tables 3 and 4; Fig. 4). During the QW state, 55 to 62% of the annual recharge of soil moisture took place, with 65 to 82% of total recharge occurring in the deeper soil horizons (>40 cm). About 206 and 141 mm of water were added to the soil profile during the recharge period (WU and QW states) in 2007–2008 and 2008–2009, respectively. During the FW state,

Table 3. Hydrologic water balance in the experimental catchment: rainfall, outflow, and change in storage for the 2007–2008 water year.

Flux	Fall wet-up 20 Sept.–16 Dec.	Quasi-wet 16 Dec.–27 Jan.	Full wet 27 Jan–1 Mar.	Dry-down 1 Mar.–6 June	Summer dry 6 June–3 Oct.	Total
	mm					
Rainfall	139	211	112	27	0	489
Stream discharge	0	12	35	0	0	47
Evapotranspiration†	45	39	21	159	33	296
Deep seepage	0	47	61	0	0	108
Change in storage‡						
0–20 cm	39	16	−2	−35	−11	7
20–40 cm	26	23	−2	−32	−8	8
40–65 cm	15	37	−1	−29	−8	14
65 cm to Cr or R	14	37	0	−36	−7	9
Profile	94	113	−5	−132	−32	38

† Evapotranspiration (ET) was calculated based on the difference between the other fluxes. In the quasi-wet and full-wet states, ET was considered to be due to canopy interception (23%) and grass interception (10%) of the rainfall.
‡ Deep seepage during quasi-wet and full-wet states was estimated based on the difference between the other fluxes.

Table 4. Hydrologic water balance in the experimental catchment: rainfall, outflow, and change in storage for the 2008–2009 water year.

Flux	Fall wet-up 2 Oct.–20 Dec.	Quasi-wet 20 Dec.–20 Feb.	Full wet 20 Feb.–8 Mar.	Dry-down 8 Mar.–6 June	Summer dry 1 June–3 Oct.	Total
	mm					
Rainfall	197	127	189	97	0	610
Stream discharge	0	7	63	0	0	70
Evapotranspiration†	148	24	35	215	56	478
Deep seepage	0	3	83	0	0	86
Change in storage‡						
0–20 cm	30	5	1	−28	−21	−12
20–40 cm	14	12	1	−26	−3	−3
40–65 cm	3	30	2	−29	−19	−13
65 cm to Cr or R	1	46	4	−36	−13	2
Profile	48	93	8	−118	−56	−26

† Evapotranspiration (ET) was calculated based on the difference between the other fluxes. In the quasi-wet and full-wet states, ET was considered to be due to canopy interception (23%) and grass interception (10%) of the rainfall.
‡ Deep seepage during quasi-wet and full-wet states was estimated based on the difference between the other fluxes.

there was no appreciable change in soil water storage for the soil profile overall.

The 2007–2008 water year ended with a surplus of 38 mm relative to the beginning of the water year, which resulted in less water needed to reach the FW state in the 2008–2009 water year (Tables 3and 4). The DD state is marked by a high rate of soil water loss as warm temperatures result in high ET rates from annual grasses and oaks. There was a gradual water loss in the SD state, probably due to oak transpiration and possibly a small amount of evaporation from the soil surface. The SWC decreased by 164 and 175 mm from the FW state to the end of the SD state, equivalent to 164- and 175-mm changes in water storage for 2007–2008 and 2008–2009, respectively (Tables 3 and 4). The overall change in the annual soil water storage was 38 mm in 2007–2008 and −26 mm in 2008–2009.

The two unknowns in the water balance calculation for each of the five soil moisture states were ET and deep seepage. We partitioned these two components based on the assumption that all measured soil water losses in excess of recharge during the WU, DD, and SD states were due to ET. During the QW and FW states (mid-December–February), we assumed that transpiration from vegetation was minimal and that evaporation was equal to canopy interception by trees (23% interception across 66% of the watershed) and grasslands (10% interception across 34% of the watershed) (Dahlgren et al., 1997). We assigned the water loss in excess of the estimated ET during the QW and FW states to deep seepage. Based on these assumptions, ET for the entire water year was 296 and 484 mm in 2007–2008 and 2008–2009, respectively. These ET values are consistent with the range of 295 to 536 mm estimated or measured for similar Sierra Nevada foothill sites (Lewis et al., 2000; Baldocchi and Xu, 2007). From 80 to 88% of the estimated ET occurred during the WU, DD, and SD states when no streamflow occurred. This left only 12 to 20% of the estimated ET during the winter when transpiration by vegetation was minimal and canopy interception was the primary mechanism for water loss to the atmosphere. Of the 323 and 316 mm of precipitation in 2007–2008 and 2008–2009, respectively, during the QW and FW states, a total of 108 and 101 mm (33 and 32%) of water recharged the soil, 47 and 70 mm (15 and 22%) contributed to streamflow, 60 and 59 mm (19 and 19%) was assigned to vegetation interception and evaporation, and 108 and 86 mm (33 and 27%) was attributed to deep seepage (Tables 3 and 4).

For the entire water year, 9.6% (47 mm) and 11.5% (70 mm) of the total rainfall left the catchment as streamflow in 2007–2008 and 2008–2009, respectively. Of this total streamflow, 75 and 90% occurred during the FW state in 2007–2008 and 2008–2009, respectively. This runoff/rainfall ratio was low compared with an adjacent perennial stream where runoff ranged from 19 to 76% (mean = 44%) of precipitation during a 17-yr period (Lewis et al., 2000). The lower runoff in our catchment may, in part, be due to greater deep seepage, which we estimated to be 2.3 and 1.2 times greater than streamflow in 2007–2008 and 2008–2009, respectively.

Interestingly, once the FW state was achieved in our study, a greater fraction of the rainfall was lost as streamflow. This was probably a result of drainage of the free water held between saturation and field capacity. Free water is subject to flow by gravitational forces, resulting in subsurface lateral flow through macropores in sloping terrain. The flashy nature of the stream hydrograph supports this hypothesis that a portion of the soil moisture storage is rapidly supplied to streams. Thus, the amount of rainfall during the FW

state is an important consideration for streamflow generation and comparisons of runoff/rainfall ratios.

Rainfall occurring during the DD period was largely consumed by ET, with no appreciable streamflow generation. During the DD and SD states, the decrease in soil water storage was very similar between the 2 yr, 164 vs. 175 mm for 2007–2008 and 2008–2009, respectively, yet the estimated 484 mm of ET in 2008–2009 was appreciably higher than the 296 mm of ET in 2007–2008. The major difference between years was an additional 128 mm of rainfall that occurred during the WU and DD states of the 2008–2009 water year, which are periods of time when evaporative demands are high. Thus, in addition to the total annual rainfall amount, the seasonality of precipitation has a strong effect on the annual magnitude of ET and streamflow.

Factors that Influence Soil Water Content at the Catchment Scale

In terms of catchment-scale management and hydrologic modeling, it is important to understand the factors affecting the SWC and their subsequent effects on streamflow dynamics. Figures 5–8 illustrate the relationships of tree canopy, the presence or absence of a claypan, solar radiation, and CTI with SWC for the near-surface biomantle and the subsurface argillic horizon within each soil moisture state.

Relationship between Oak Canopy Cover and Soil Water Content

A significant tree canopy influence on SWC was observed for the biomantle during the fall WU state. Soils with open and partial canopy coverage had higher SWCs than those beneath a tree canopy (Fig. 5a). Canopy interception by trees can reduce soil water inputs by 15 to 23% beneath blue oak canopies (Dahlgren and Singer, 1994), and therefore rewetting of the upper soil profile is slower under oak trees during the WU state. Similarly, there was a lag in soil recharge in the subsurface argillic horizon beneath tree canopies during the QW state as the advance in the wetting front was attenuated by canopy interception (Fig. 5b). There was no canopy effect on SWC in the FW state at either depth because the soils were much closer to their storage capacity and the trees were dormant.

During the SD state, deeper soil layers beneath the canopy dried more quickly due to preferential removal of water from these horizons by the deeply rooted oak trees. The SWC remained lower beneath the canopy throughout the SD period; however, the difference was not significant due to the high variability found in open grassland positions. In contrast, no differences in SWC were observed in the upper soil horizons between open, partial, and closed canopy areas in the DD and SD states. This was probably due to the presence of annual grasses with a shallow rooting structure (~30 cm) occurring beneath the canopy and in open grassland areas (Baldocchi et al., 2004; Huang, 1997; Hodnett et al., 1995).

Relationship between Claypan Presence and Soil Water Content

In the near-surface biomantle, a significantly higher SWC was found in soils with claypans during the FW state (Fig. 6a). This relationship reflects perched water table dynamics associated with soils having claypans, where saturation extended into the upper soil layers during storm events once subsoil horizons were saturated. During this state, a surplus in storage occurred and subsurface lateral flow became prominent. This occurred preferentially in the Palexeralfs, which have claypans that restrict downward flow, promoting subsurface lateral flow (Dahlgren and Singer, 1994; O'Geen et al., 2010). In fact, the only factor significantly influencing the SWC of the biomantle during the FW state (the period of greatest streamflow) was the presence of a claypan (Table 5). While most current hydrologic models rely on topographic indices to predict water flow, our results demonstrate that soil stratigraphy is important for predicting hydrologic behavior at the catchment scale.

In the subsurface argillic horizon, the presence of a claypan had a significant effect on the SWC during the deep recharge and utilization periods (QW, FW, and DD states) (Fig. 6b). In the QW and FW states, the greater water holding capacity of the claypan contributed to the observed higher SWC in the Palexeralfs. The presence of a claypan also increased water storage during the DD state. Therefore, claypan soils have a significant impact on deep water storage in semiarid systems, where oak trees are highly dependent on stored water to survive throughout the SD period. Studies have shown that oak trees possess strategies to cope with water stress by accessing deep groundwater (Lewis and Burgy, 1964; Miller et al., 2010) and possibly redistributing water from deep to near-surface horizons by hydraulic lift (Millikin Ishikawa and Bledsoe, 2000). We did not see evidence of hydraulic lift in our data set, however.

Relationship between Solar Radiation and Soil Water Content

Locations with high solar radiation values (e.g., south-facing slopes) had significantly more water in the near-surface biomantle than those with lower solar radiation (north-facing slopes) during the SD state (Fig. 7a). One contributing factor was the lower tree density occurring on the south-facing slopes. In addition, Ng and Miller (1980) found that annual grasses died earlier on the hotter south-facing slopes. Because transpiration ceases as annual grasses die, the only force acting in open grassland that extracts water during this state is evaporation from the soil surface and localized transpiration by oak trees. Moreover, a dry surface soil layer creates a hydraulic disconnect between the soil surface and the remainder of the soil profile.

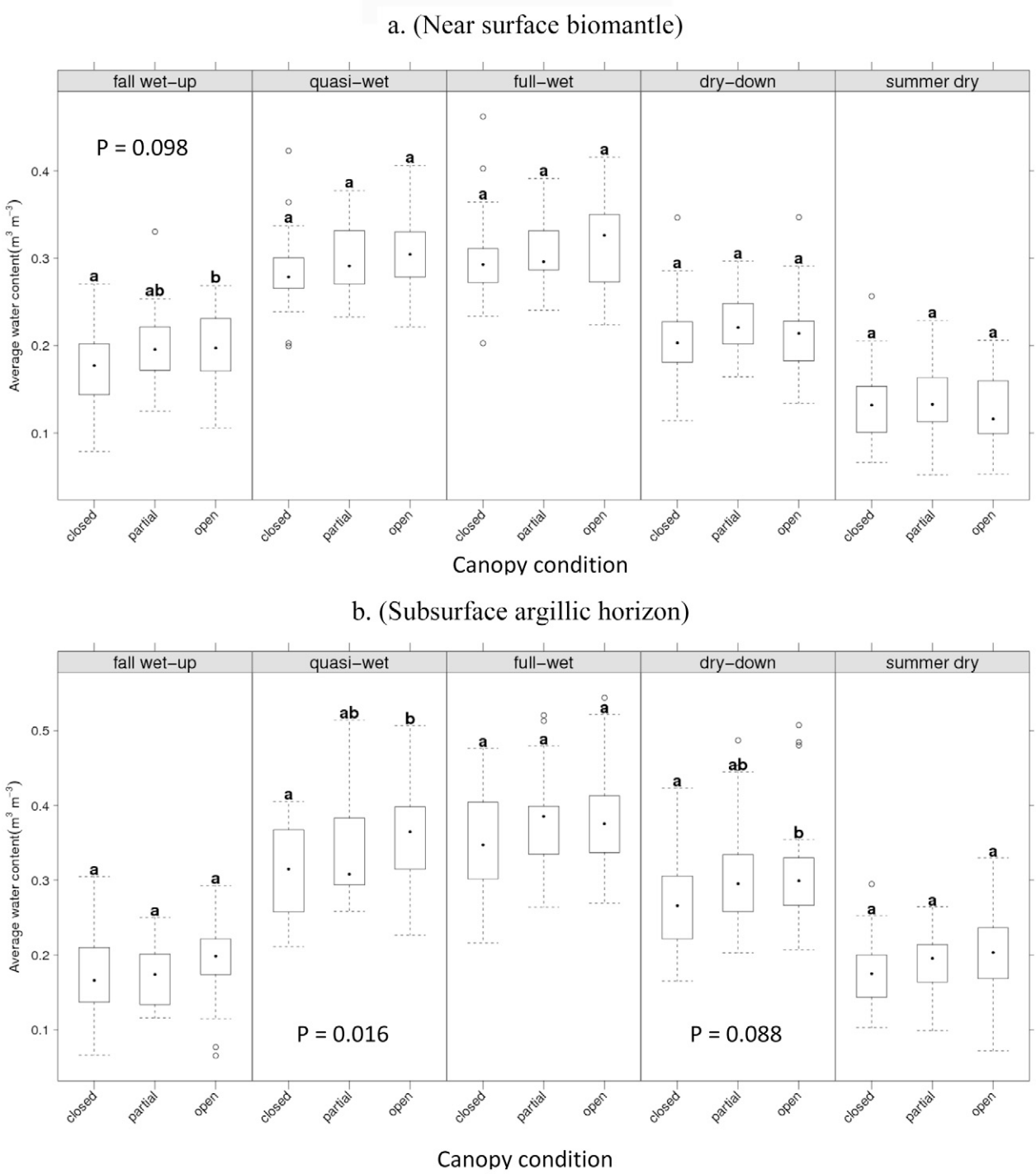

Fig. 5. Boxplot of mean SWC conditional on the nominal combination of season and canopy in the upper (a) and lower (b) soil layer. The dot in each box is the median, the boxes define the hinge (25–75% quartile) and the line is 1.5 times the hinge. Points outside this interval are represented as circles. In a given season, different letters between treatments represent a significant difference.

This lack of conductivity greatly reduces unsaturated flow in the upper soil profile and helps preserve water beneath the surface soil layer (Robinson et al., 2010). Interestingly, solar radiation had no effect on soil moisture in the biomantle for the rest of the hydrologic states; significant differences were present, however, in the subsurface argillic horizon.

In the subsurface argillic horizon, the average SWC was greater in locations with lower solar radiation (north-facing slopes) during the entire deep recharge and utilization period (QW through DD states) (Fig. 7b). Because oak trees are dormant during the QW and FW states, the greater water content of the north-facing areas may be attributed to differences in infiltration. Hunckler and Schaetzl (1997) found that soils with north- to

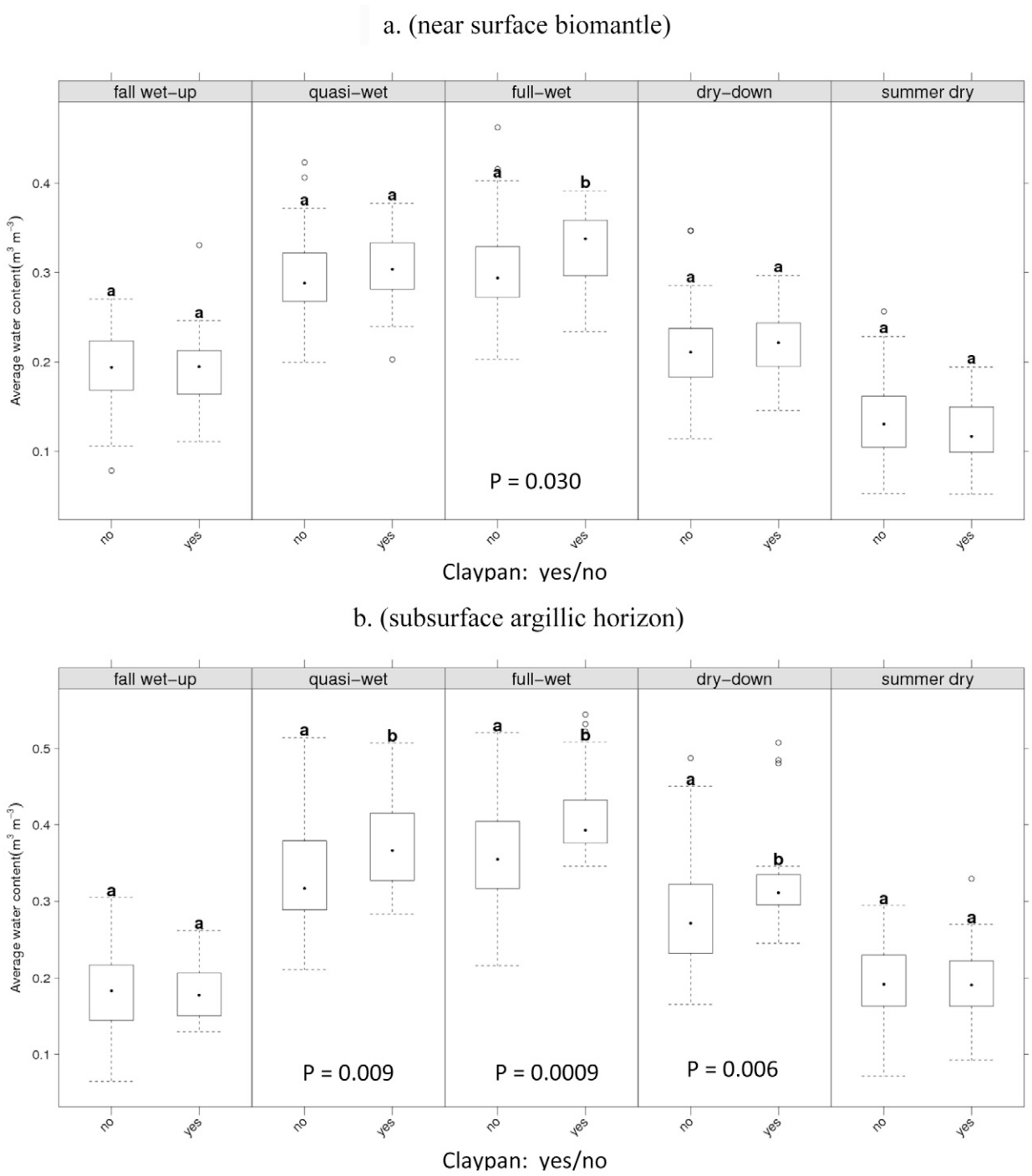

Fig. 6. Boxplot of mean SWC conditional on the nominal combination of season and presence or absence of a semi-permeable layer (claypan) in the upper (a) and lower (b) soil layer. The dot in each box is the median, the boxes define the hinge (25–75% quartile) and the line is 1.5 times the hinge. Points outside this interval are represented as circles. In a given season, different letters between treatments represent a significant difference.

northeast-facing slopes had more strongly developed structure resulting in greater water infiltration compared with south- to southwest-facing soils. Similarly, preferential flow paths associated with tree root channels can contribute increased water flow to subsurface horizons. Theoretically, the microenvironmental differences described above could play an important role in causing wetter north-facing slopes in winter months (Finney et al., 1962; Qiu et al., 2001). Another factor that may contribute to the higher SWC observed in north-facing areas during the QW and FW states is bedrock topography and permeability, which can direct water flow preferentially (Freer et al., 2002). In addition, claypans tend to be more abundant on north-facing slopes, thereby maintaining higher SWC values in surface horizons during the wettest months (Table 5).

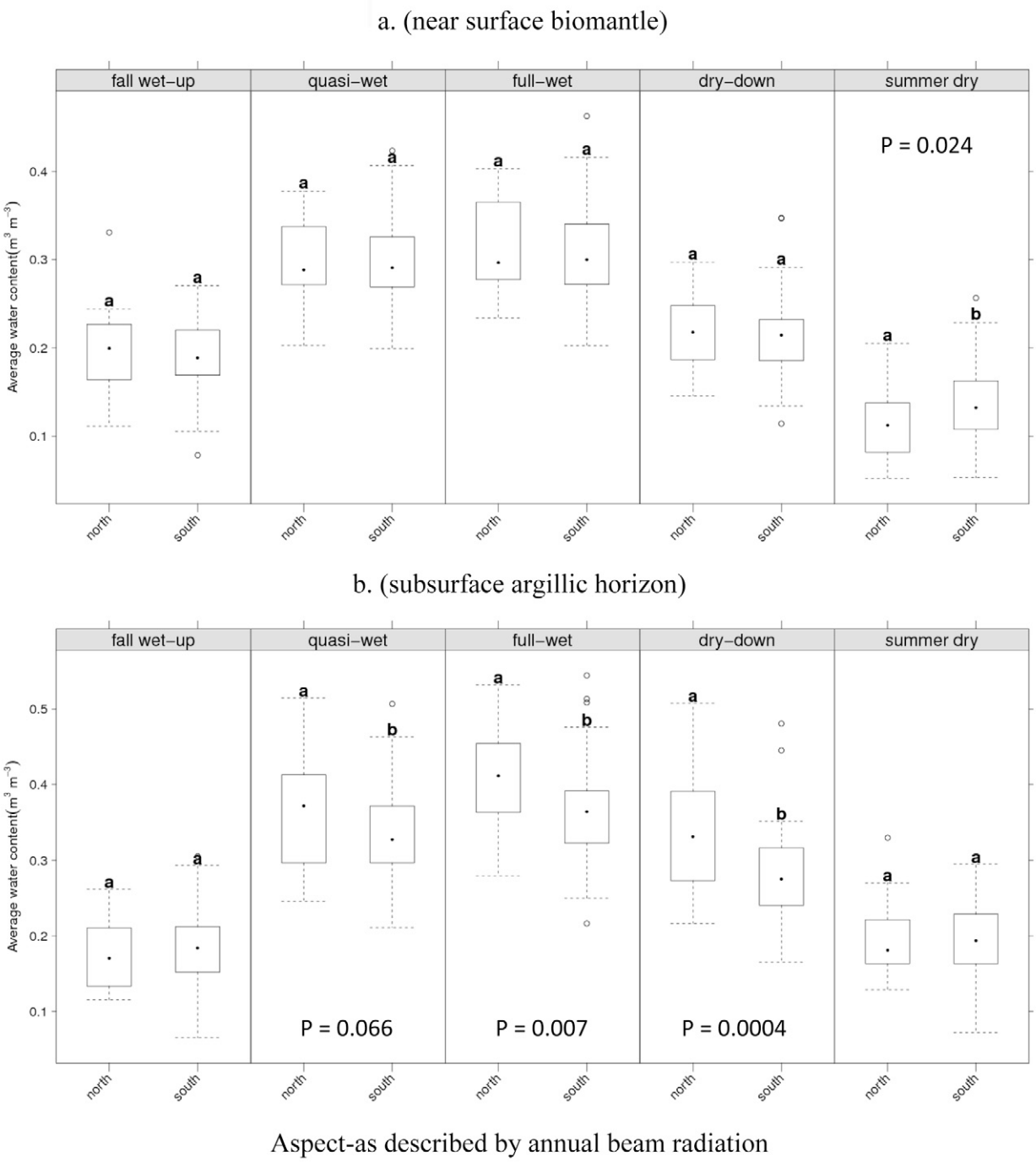

Fig. 7. Boxplot of mean SWC conditional on the nominal combination of season and solar radiation in the upper (a) and lower (b) soil layer. The dot in each box is the median, the boxes define the hinge (25–75% quartile) and the line is 1.5 times the hinge. Points outside this interval are represented as circles. In a given season, different letters between treatments represent a significant difference. Insolation values ranging from 37510 to 57878 MJ m^{-2} yr^{-1} were binned into "north" and those ranging from 57879 to 71660 MJ m^{-2} yr^{-1} as "south".

Relationship between Compound Topographic Index and Soil Water Content

The CTI is a common topographically derived proxy for water accumulation across the landscape. In the upper 40 cm, no relationship between topography and SWC was observed, even during the FW state (Fig. 8a). Any potential effect should have been most evident during the FW state because this was the period of greatest flow in the surface horizons. Near-surface saturation was infrequent and of short duration, occurring when the water table reached the soil surface during storm events. As a result, the SWC was highly variable in the surface horizons during the wet seasons and the temporal variability in moisture content complicates statistical comparisons. The lack of a topographic relationship for SWC in the upper 40 cm and the significant relationship

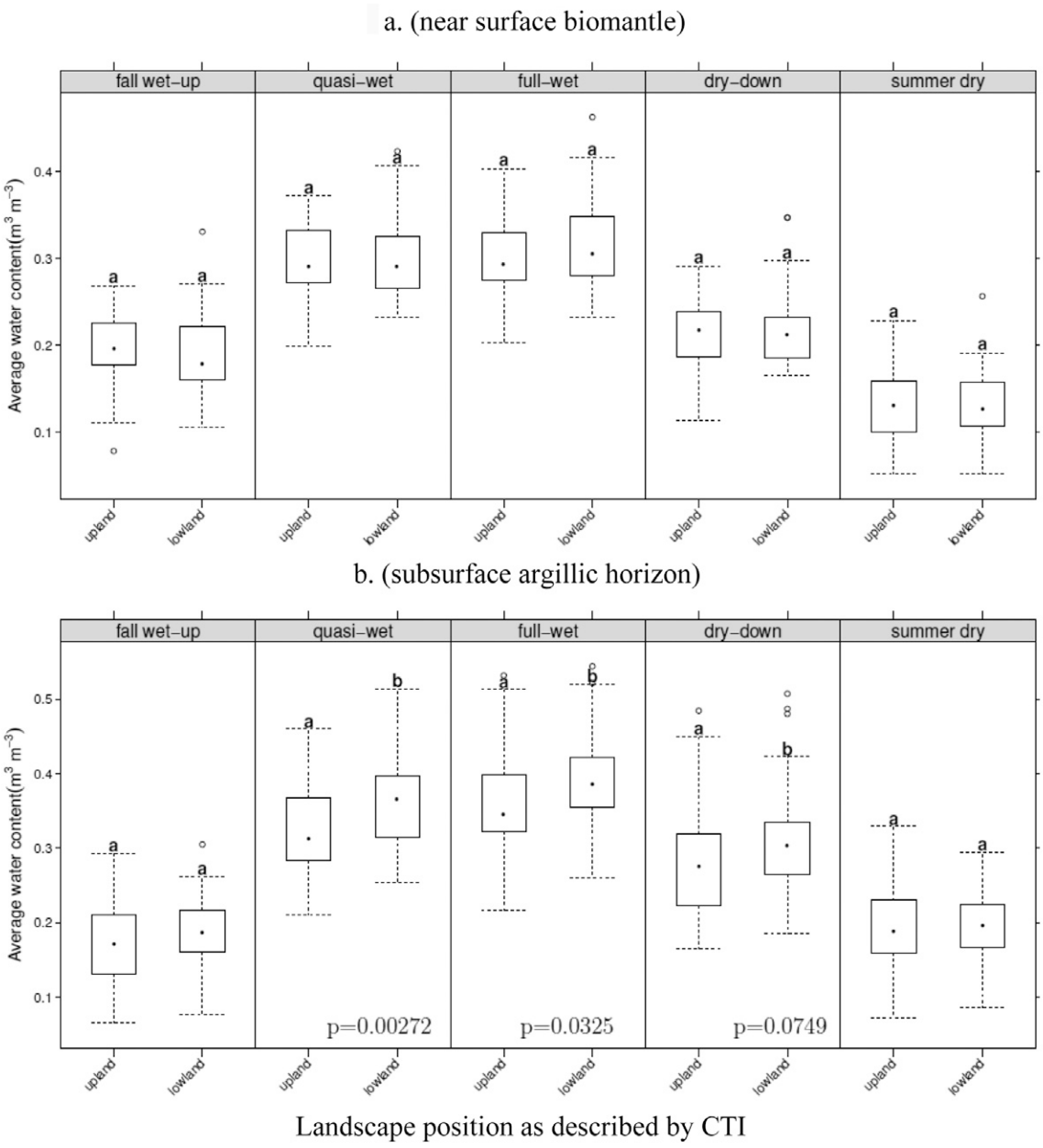

Fig. 8. Boxplot of mean SWC conditional on the nominal combination of season and the topographic index (CTI) in the upper (a) and lower (b) soil layer. The dot in each box is the median, the boxes define the hinge (25–75% quartile) and the line is 1.5 times the hinge. Points outside this interval are represented as circles. In a given season, different letters between treatments represent a significant difference. CTI was used to classify locations as either: "lowland" (CTI ranging from 4.45 to 6.13) or "upland" (CTI ranging from 6.13 to 10.38).

between SWC and claypan soils indicate that soil stratigraphy is a more important attribute for describing the near-surface hydrology in these settings (Table 5). This suggests that watershed hydrologic models that depend on topographic indices to describe water flow may have some limitations in describing hydrologic flow paths.

On the other hand, soils in "lower" landscape positions (high CTI) had a greater SWC in the subsurface argillic horizon during the QW, FW, and DD states (Fig. 8b). During the QW and FW states, water moved downslope to lower landscape positions. Several studies have documented greater SWC in landscape positions with large contributing areas (Ceballos and Schnabel, 1998; Robinson et al., 2010). In contrast, Tromp-van Meerveld and McDonnell (2006) found no difference in SWC between upslope and lower positions during the wet period; however, their catchment was in a humid setting and highly dependent on bedrock topography. During the DD state, lower landscape positions had higher average SWCs, reflecting greater pooling of water during the wet states. Similar observations were made by Tromp-van Meerveld and McDonnell (2006), where the average SWC in upslope areas was less than that of lower landscape positions during the dry-down and dry states.

Table 5. Seasonal occurrence of factors that significantly increased soil water storage.

Depth	Fall wet-up	Quasi-wet	Full wet	Dry-down	Summer dry
Biomantle	open canopy	none	claypan	none	south aspect
Subsurface argillic	none	open canopy claypan north aspect lowland positions	claypan north aspect lowland positions	open canopy claypan north aspect lowland positions	none

General Differences between Upper and Lower Soil Layers

The results of this study clarify the relative importance of the water storage capacity of deeper soil horizons and water transmission ability of surface horizons. During the period of significant soil water exchange (QW, FW, and DD states), the effects of canopy, claypans, solar radiation, and topography occurred mostly in lower soil horizons, mainly due to the fact that these horizons had a higher clay content and therefore retained water for a longer period of time (Fernandez-Illescas et al., 2001; Weng and Luo, 2008). Lower horizons also had the largest density of oak roots, which extracted water throughout the DD and SD states. The SWC in the upper soil horizons fluctuated on seasonal (wet to dry season) and short-term (rainfall event) time scales as opposed to the lower soil horizons, which showed primarily seasonal soil water storage fluctuations. In general, lower soil horizons responded to rainfall after a surplus occurred in the upper soil layers. Hodnett et al. (1995) reported similar results, with soil water storage in the upper portion of the profile almost identical under forest and pasture, in contrast to the lower portion of the profile, where the greatest differences were seen. Similarly, Tromp-van Meerveld and McDonnell (2006) highlighted the importance of soil depth observations to understand the relationships between SWC, vegetation patterns, and topography.

Seasonality

Seasonal swings in SWC were governed by interactions between climate, vegetation, topography, and soil properties. Plant water availability varied according to precipitation patterns and solar radiation intensity, factors with significant seasonal changes. In the WU state, canopy interception was the primary factor contributing to differences in SWC. All other factors were not significant, mainly because soil water recharge was limited to the upper layer and annual grasses were largely dormant (Table 5).

During the QW state, all the studied factors become important to water storage: canopy, claypan, solar radiation, and topography. These relationships were primarily observed in the lower soil profile, which is the main reservoir of soil water. Plants were largely inactive due to cold temperatures, and the low ET allowed soil water recharge to occur. In the FW state, soil water surplus occurred. Excess water was transported as subsurface lateral flow, primarily through the porous A and AB horizons, as the perched water table extended upward from the claypan into these horizons. Lateral flow paths were only observed during the FW state once a perched water table developed above the claypan. This highlights the rationale for dividing the wet period into the QW when deep storage occurs and FW state when lateral flow is initiated.

The DD state was marked by active growth of both annual grasses and oak trees. This is the most important state in terms of vegetative growth (80% of the stored water is taken up by plants in this state). Similar to the QW state, no significant relationships were seen between the SWC in the upper 40 cm with respect to all factors examined. The permeable nature of the upper 40 cm throughout the watershed coupled with the presence of annual grasses in all landscape positions may be why this depth behaved uniformly during DD. In the subsoil, the SWC was significantly lower in closed canopy areas where water was taken up by oak trees during DD. Claypan soils were important for water storage, as were lowland positions and north-facing slopes, all of which stored more water during this period. In the SD state, only solar radiation showed a relationship with SWC in the near-surface biomantle. In the subsurface argillic horizon, there was no relationship between SWC and any factor during the two driest states, SD and WU.

Study Implications

Soils in Mediterranean climates can store a large portion of precipitation as soil moisture, which regulates hydrologic flow paths and streamflow. This study demonstrated that streamflow generation was largely limited to the wet winter months and occurred only after soils approached saturation throughout the watershed. In terms of water quality, the transport of contaminants associated with cattle grazing (*Escherichia coli*, dissolved organic C, and nutrients) is most probable during the FW state when the soils are saturated and rapid subsurface lateral flow through the near-surface horizons limits soil filtering and retention of these constituents. Thus, grazing management can be coordinated with the hydrologic states to minimize contaminant export to surface waters.

This study further demonstrated that vegetation (tree vs. grassland), claypan occurrence, aspect, and surface topographic features all have an influence on the soil moisture status and subsequent catchment hydrology. Thus, catchment-scale hydrologic models based solely on surface topography will not fully capture dynamic changes in hydrologic processes. Knowledge of soil stratigraphy (e.g., claypan distribution) is important for understanding catchment hydrology, especially the occurrence of subsurface lateral flow dynamics. Soils were shown to provide a large water buffering capacity between storms that reduced peak flows and downstream flooding potential. Vegetation management (tree removal and grazing intensity) may alter the soil moisture dynamics, however, resulting in greater runoff and higher peak flows.

The runoff/rainfall ratio was shown to be affected by both the total annual precipitation and the distribution of rainfall throughout the year. Because significant runoff occurs during winter wet soil moisture states when ET is low, additional rainfall during this time will result in greater runoff. In contrast, precipitation during the WU and SD states will largely be lost as ET. Thus, temporal shifts in the precipitation pattern as a result of possible climate change may have the greatest impact on future stream runoff patterns in Mediterranean oak woodlands.

Acknowledgments

We thank Jiayou Deng, Sarah Hentges Ceron, Dylan Beaudette, and the UC Sierra Foothil Research and Extension Center for their lab and field support. This study was funded in part by the California State Water Resources Control Board (Agreement no. 04-120-555-01) and the Kearney Foundation of Soil Science.

References

Baldocchi, D.D., and L. Xu. 2007. What limits evaporation from Mediterranean oak woodlands—The supply of moisture in the soil, physiological control by plants or the demand by the atmosphere? Adv. Water Resour. 30:2113–2122. doi:10.1016/j.advwatres.2006.06.013

Baldocchi, D.D., L. Xu, and N. Kiang. 2004. How plant functional-type, weather, seasonal drought, and soil physical properties alter water and energy fluxes of an oak–grass savanna and an annual grassland. Agric. For. Meteorol. 123:13–39. doi:10.1016/j.agrformet.2003.11.006

Beaudette, D.E., and A.T. O'Geen. 2009. Quantifying the aspect effect: An application of solar radiation modeling for soil survey. Soil Sci. Soc. Am. J. 73:1345–1352. doi:10.2136/sssaj2008.0229

Beiersdorfer, C.L. 1987. Metamorphic petrology of the Smartville complex, northern Sierra Nevada foothills. M.S. thesis. Univ. of California, Davis.

Black, P. 1996. Watershed hydrology. CRC Press, Boca Raton, FL.

Ceballos, A., and S. Schnabel. 1998. Hydrological behaviour of a small catchment in the *dehesa* landuse system (Extremadura, SW Spain). J. Hydrol. 210:146–160. doi:10.1016/S0022-1694(98)00180-2

Chamran, F., P. Gessler, and O. Chadwick. 2002. Spatially explicit treatment of soil-water dynamics along a semiarid catena. Soil Sci. Soc. Am. J. 66:1571–1583. doi:10.2136/sssaj2002.1571

Dahlgren, R., W. Horwath, K. Tate, and T. Camping. 2003. Blue oak enhance soil quality in California oak woodlands. Calif. Agric. 57:42–47. doi:10.3733/ca.v057n02p42

Dahlgren, R., and M. Singer. 1994. Nutrient cycling in managed and unmanaged oak woodland–grass ecosystems. Final Rep., Integrated Hardwood Range Management Program. Land Air Water Resour. Pap. 100028. Tech. Rep. Univ. of California, Davis.

Dahlgren, R.A., M.J. Singer, and X. Huang. 1997. Oak tree grazing impacts on soil properties and nutrients in a California oak woodland. Biogeochemistry 39:45–64. doi:10.1023/A:1005812621312

Fernandez-Illescas, C.P., A. Porporato, F. Laio, and I. Rodriguez-Iturbe. 2001. The ecohydrological role of soil texture in a water-limited ecosystem. Water Resour. Res. 37:2863–2872. doi:10.1029/2000WR000121

Finney, H.R., N. Holowaychuk, and M.R. Heddleson. 1962. The influence of microclimate on the morphology of certain soils of the Allegheny Plateau of Ohio. Soil Sci. Soc. Am. J. 26:287–292. doi:10.2136/sssaj1962.03615995002600030026x

Freer, J., J. McDonnell, K. Beven, N. Peters, D. Burns, R. Hooper, B. Aulenbach, and C. Kendall. 2002. The role of bedrock topography on subsurface storm flow. Water Resour. Res. 38:1269–1285. doi:10.1029/2001WR000872

Grayson, R., A. Western, F. Chiew, and G. Bloschl. 1997. Preferred states in spatial soil moisture patterns: Local and nonlocal controls. Water Resour. Res. 33:2897–2908. doi:10.1029/97WR02174

Hayes, W., and G. Koch. 1984. Constructing and analyzing area-of-influence polygons by computer. Comput. Geosci. 10:411–431. doi:10.1016/0098-3004(84)90042-6

Hodnett, M., L. Silva, H. Rocha, and R. Cruz Senna. 1995. Seasonal soil water storage changes beneath central Amazonian rainforest and pasture. J. Hydrol. 170:233–254. doi:10.1016/0022-1694(94)02672-X

Huang, X. 1997. Watershed hydrology, soil, and biogeochemistry in an oak woodland annual grassland ecosystem in Sierra foothills, California. Ph.D. diss. Univ. of California, Davis.

Hunckler, R.V., and R.J. Schaetzl. 1997. Spodosol development as affected by geomorphic aspect, Baraga County, Michigan. Soil Sci. Soc. Am. J. 61:1105–1115. doi:10.2136/sssaj1997.03615995006100040017x

Jackson, L.E., R. Strauss, M. Firestone, and J. Bartolome. 1990. Influence of tree canopies on grassland productivity and nitrogen dynamics in deciduous oak savanna. Agric. Ecosyst. Environ. 32:89–105. doi:10.1016/0167-8809(90)90126-X

Joffre, R., and S. Rambal. 1993. How tree cover influences the water balance of Mediterranean rangelands. Ecology 74:570–582. doi:10.2307/1939317

Kizito, F., C. Campbell, G. Campbell, D. Cobos, B. Teare, B. Carter, and J. Hopmans. 2008. Frequency, electrical conductivity and temperature analysis of a low-cost capacitance soil moisture sensor. J. Hydrol. 352:367–378.

Lewis, D., M. Singer, R. Dahlgren, and K. Tate. 2000. Hydrology in a California oak woodland watershed: A 17-year study. J. Hydrol. 240:106–117. doi:10.1016/S0022-1694(00)00337-1

Lewis, D.C., and R.H. Burgy. 1964. The relationship between oak tree roots and groundwater in fractured rock as determined by tritium tracing. J. Geophys. Res. 69:2579–2588. doi:10.1029/JZ069i012p02579

Lindstrom, M., and D. Bates. 1990. Nonlinear mixed effects models for repeated measures data. Biometrics 46:673–687. doi:10.2307/2532087

Major, J. 1988. California climate in relation to vegetation. p. 11–74. *In* M.G. Barbour and J. Major (ed.) Terrestrial vegetation of California Spec. Publ. 9. Calif. Native Plant Soc., Berkeley.

McNamara, J.P., D.G. Chandler, M. Seyfried, and S. Achet. 2005. Soil moisture states, lateral flow, and streamflow generation in a semi-arid, snowmelt-driven catchment. Hydrol. Processes 19:4023–4038. doi:10.1002/hyp.5869

Miller, G.R., X. Chen, D. Baldocchi, and Y. Rubin. 2010. Groundwater uptake by woody vegetation in a Mediterranean oak savanna. Water Resour. Res. 46:W10503. doi:10.1029/2009WR008902

Millikin Ishikawa, C., and C. Bledsoe. 2000. Seasonal and diurnal patterns of soil water potential in the rhizosphere of blue oaks: Evidence for hydraulic lift. Oecologia 125:459–465. doi:10.1007/s004420000470

Milly, P.C.D. 1994. Climate, soil water storage, and the average annual water balance. Water Resour. Res. 30:2143–2156. doi:10.1029/94WR00586

Moehrlen, C., G. Kiely, and M. Pahlow. 1999. Long term water budget in a grassland catchment in Ireland. Phys. Chem. Earth, Part B 24:23–29.

Moore, I., P. Gessler, G. Nielsen, and G. Peterson. 1993. Soil attribute prediction using terrain analysis. Soil Sci. Soc. Am. J. 57:443–452. doi:10.2136/sssaj1993.03615995005700020026x

Moore, I.D., R.B. Grayson, and A.R. Ladson. 1991. Digital terrain modeling: A review of hydrological, geomorphological, and biological applications. Hydrol. Processes 5:3–30. doi:10.1002/hyp.3360050103

National Geographic Society. 2010. Water: Our thirsty world—A special issue. National Geographic, April.

Ng, E., and P.C. Miller. 1980. Soil moisture relations in the southern California chaparral. Ecology 61:98–107. doi:10.2307/1937160

O'Geen, A.T., R.A. Dahlgren, A. Swarowsky, K.W. Tate, D.J. Lewis, and M.J. Singer. 2010. Research connects soil hydrology and stream water chemistry in California oak woodlands. Calif. Agric. 64:78–84. doi:10.3733/ca.v064n02p78

Pinheiro, J., D. Bates, S. DebRoy, D. Sarkar, and the R Development Core Team. 2009. nlme: Linear and nonlinear mixed effects models. R package version 3.1-96. Available at cran.r-project.org/web/packages/nlme/index.html (verified 13 July 2011). Inst. for Stat. and Math., Vienna Univ. of Econ. and Business, Vienna, Austria.

Pistocchi, A., F. Bouraoui, and M. Bittelli. 2008. A simplified parameterization of the monthly topsoil water budget. Water Resour. Res. 44:W12440. doi:10.1029/2007WR006603

Qiu, Y., B. Fu, J. Wang, and L. Chen. 2001. Soil moisture variation in relation to topography and land use in a hillslope catchment of the Loess Plateau, China. J. Hydrol. 240:243–263. doi:10.1016/S0022-1694(00)00362-0

R Development Core Team. 2009. R: A language and environment for statistical computing. R Foundation for Stat. Comput., Vienna, Austria.

Robinson, D.A., I. Lebron, and J.I. Querejeta. 2010. Determining soil–tree–grass relationships in a California oak savanna using eco-geophysics. Vadose Zone J. 9:528–536. doi:10.2136/vzj2009.0041

Snyder, R., D. Henderson, W. Pruitt, and A. Dong. 1985. California irrigation management information system. Final Rep. Land, Air, and Water Resour. Pap. 10013a,b,c. Tech. Rep. Dep. of Land, Air, and Water Resour., Univ. of California, Davis.

Tromp-van Meerveld, H.T., and J. McDonnell. 2006. On the interrelations between topography, soil depth, soil moisture, transpiration rates and species distribution at the hillslope scale. Adv. Water Resour. 29:293–310. doi:10.1016/j.advwatres.2005.02.016

Weng, E., and Y. Luo. 2008. Soil hydrological properties regulate grassland ecosystem responses to multifactor global change: A modeling analysis. J. Geophys. Res. 113:G03003. doi:10.1029/2007JG000539